TRANSLATION

TITLE : — as translated into ENGLISH

KKB - VENT CLEARING WITH THE PERFORATED-PIPE QUENCHER

KKB - FREIBLASEN MIT D

AUTHOR/S/ : DR.

DR.

SOURCE : KWU

12

(PP

Translated

PROPRIETARY INFORMATION

This document has been made NON-PROPRIETARY by the deletion of that information which was classified as PROPRIETARY by KRAFTWERK UNION AG (KWU).

The PROPRIETARY information deletions are so noted throughout the report where indicated by

a) Use of the term KRAFTWERK UNION AG PROPRIETARY INFORMATION.

b) Use of blocked out areas by cross hatch bands in the report text and figures/tables, e.g.

i) ...." with a mass flow density of [redacted] Kg/m^2s...";

ii) [redacted] mm

iii) ...." should be kept below [redacted] atm."

iv) [redacted]

8/17/78

Frankfurt (Main) — Place
12 October 1973 — Date

Technical Report KWU/E3-2796

File number E3/E2 Dr. Be/bf

Kraftwerk Union
R 113
Department

Author Dr. Becker
Dr. Koch
Countersignature /s/

Title: KKB - Vent clearing with the perforated-pipe quencher

Pages of text	53
Figures	48
Circuit diagrams	
Diagr./oscillogr.	
Tables	9
Reference list	1

Key words (max. 12) to identify the report's content:

Relief system, suppression chamber, load during water and air expulsion

Summary: This report contains the essential data for the dimensioning of the mount of the relief system from the valve and bracing of the relief system to the bottom of the suppression chamber. The pressure amplitudes at the bottom during air expulsion are also investigated.

The following quantities are indicated:
- the design parameters of the system,
- the pressure build-up in the pipe during water expulsion,
- the pressure oscillations during air expulsion,
- the transverse forces on the quencher.

The information is based on tests in the Mannheim Central Power Station (GKM) with the perforated-pipe quencher HS 1.

/s/ Dr. Becker
/s/ Mr. Hoffmann
/s/ Mr. Knapp
/s/ Dr. Kraemer
/s/ Dr. Melchior
/s/ Mr. Meyer
/s/ Mr. Schnabel
Author's signature

/s/ Dr. Koch — Examiner
/s/ Dr. Domin — Classifier
II — Class

For information (cover sheet only):

Distribution list:
1x KWU/GA 19 Erl
1x /PSW 22 Ffm
1x E 3-Bibl. Gwh

NONLIABILITY CLAUSE

This report is based on the current technical knowledge of KRAFTWERK UNION AG. However, KRAFTWERK UNION AG and all persons acting in its behalf make no guarantee. In particular, they are not liable for the correctness, accuracy and completeness of the data contained in this report nor for the observance of third-party rights.

This reservation does not apply insofar as the report is delivered in fulfillment of contractual obligations, nor with respect to licensing authorities or the experts appointed by them.

KRAFTWERK UNION AG reserves all rights to the technical information contained in this report, particularly the right to apply for patents.

Further dissemination of this report and of the knowledge contained therein requires the written approval of KRAFTWERK UNION AG. Moreover, this report is communicated under the assumption that it will be handled confidentially.

DISTRIBUTION LIST (internal)

E 3 - Sekretariat
E 3/V
E 3/V 1
E 3/V 2
E 3/V 3
E 3/V 4
E 3/V 4/KWW
E 3/V 4/KKB
E 3/V 4/KKK
E 3/V 4/KKP
E 3/V 4/KKI
E 3/V 4/GKT
E 3/V 5
E 3/E
E 3/EE
E 3/E/IP
E 3/E 1
E 3/E 1/GK
E 3/E 1/GKT
E 3/E 1/GKK
E 3/E 1/EP 2 x
E 3/E 2
E 3/E 2/SA 4 x
E 3/E 3 5 x
E 3/R
E 3/R 1 2 x
E 3/R 2.
E 3/R 2/KL
E 3/R 3
E 3/R 4
E 3/R 5 2 x

TABLE OF CONTENTS

1. Introduction

KWU boiling-water reactors are equipped with a safety/relief system. By means of quick-opening valves, large amounts of steam can be condensed in the suppression chamber as water via blowdown pipes. The blowdown pipes are equipped with quenchers to limit the dynamic loads that occur.

The perforated-pipe quencher was shown to have the best blowdown geometry in an extensive testing program in the Mannheim Central Power Station (GKM) and was optimized for operational readiness. The dynamic pressures to be expected for the various operating phases with steady-state condensation are illustrated in detail in /4/. The purpose of this report is to indicate the pressures to be expected in the pipe and in the suppression chamber during vent clearing.

The physical processes during vent clearing are described and the clearing pressures are determined for various operating conditions. The pressure possible in the blowdown pipe and quencher in the most unfavorable case is [redacted] kg/cm^2 (gauge).

A detailed presentation of the experimental results makes clear the influence of parameter variations on the dynamic pressures at the bottom and walls of the suppression chamber. The values to be expected in the plant can be inferred from a comparison of parameters for the model quencher and full-scale version. This leads to pressure amplitudes which lie below

the desired maximum load of [redacted] kg/cm^2.

The maximum transverse load on the quencher, which does not exceed the specified value of [redacted] Mp, is discussed in another section of the report.

2. Description of the relief system

Figure 2.1 shows the construction, arrangement and principal dimensions of the relief system consisting of relief valves, the blowdown pipe, the perforated-pipe quencher, the support structure and the protective tube.

The blowdown pipe connects to the relief valve with a nominal width of [illegible] mm. In the suppression chamber the blowdown pipe is expanded to an inside diameter of [illegible] mm and is drawn in again to a nominal width of [illegible] mm at the water level. The submergence of the quencher, relative to the normal water level and center line of the quencher arms, is just [illegible] m.

The construction of the perforated-pipe quencher itself is shown in Figure 2.2. It is constructed with a total of [illegible] bores with [illegible] mm bore diameter. On two quencher arms which point in the same circumferential direction, thrust bores are made in the quencher ends in order to produce a circulation flow in the suppression chamber for the purpose of achieving a more uniform temperature distribution and also to apply against the bottom brace during the blowdown.

The most important dimensions and operating data of the system are compiled in Table 2.1. The indicated steam flow density relates to the actual flow rate at the reactor operating pressure. Blowdown at a reactor pressure of [illegible] bar is considered in the design.

The protective tube, the bottom brace (Figure 2.3) and the valve mount are so designed that in an assumed break of the blowdown pipe no steam is released into the air space of the suppression chamber. It should also be noted that even in the event of a break in this pipe during the clearing process, the load on the suppression chamber due to air pressure oscillations remains within the limits permissible for such a case.

3. Vent clearing process

3.1 Pressure build-up during water expulsion

Before the safety-relief valve opens, the water level in the blowdown pipe is at the same height as outside in the pool, at least until a pressure equalization prevails between the drywell and suppression chamber. After the valve opens, steam flows into the space between the valve and the water level and is mixed with the air present there. This increases the pressure in the pipe and the water slug is expelled from the blowdown pipe and quencher.

In principle, this process corresponds to the process of the plain-ended pipe /1/. The model extended for quenchers to calculate the vent clearing pressure is illustrated in the Appendix. Calculation and measurement are also compared there. We find good agreement for those tests in which the condensation rate of the inflowing steam at the pipe wall and at the water level is low. Since the condensation of steam is neglected in the vent clearing model, clearing pressures which are conservatively too high are calculated for high condensation rates.

The clearing pressures calculated in this manner for the power plant are plotted in Figure 3.1 as a function of the valve-opening time for blowdown from rated reactor pressure and from the pressure transient. It was taken into consideration that

the orifice plate following the valve in the plant produces a pressure loss which, in a conservative estimate, was assumed to be [redacted] kg/cm^2. For a blowdown from the pressure transient there results then a maximum possible pipe pressure of [redacted] kg/cm^2 (gauge) for an assumed extremely short valve-opening time of [redacted] ms, assuming also a hot pipe-wall, i.e., a negligible condensation rate.

The influence of the condensation rate on the clearing pressure for a cold blowdown pipe can be determined by an examination of the GKM tests. Figure A 5 shows good agreement of calculation and measurement for a condensation rate of [redacted]. This corresponds to [redacted] kg of condensing steam. In accordance with the larger pipe surface area in the plant, a correspondingly larger amount of condensing steam must be anticipated there. The associated clearing pressures are entered in Figure 3.1.

The pressure profile calculated for the plant up to the vent clearing times, together with the maximum conceivable peak pressure value ([redacted]), is plotted versus time in Figure 3.2. For its further time variation, this curve was extrapolated using GKM Test No. 252. Since the air volume relative to the quencher outlet area and thus also the air expulsion time is larger in this test than in the plant, a slower pressure drop to the steady-state final value is also assumed conservatively. This final

value was specified at [redacted] the expected value with steady-state condensation from rated reactor pressure and thus is also far higher than is to be expected for a blowdown from the pressure transient. The pressure profile stipulated in this manner was approximated by line segments.

3.2 Steam-air mixing

Two limiting models can be formulated for the mixing of steam and air when the steam flows into the air-filled space between the valve and water level after the valve is opened /1/:

- If we make the extreme assumption that the steam and air do not mix with each other, then the steam will push the air before it just like a piston and thereby compress it (piston model).

- In the other extreme case, we can assume an ideal mixing of steam and air (homogeneous mixing model).

In reality, a mixing gradient will have been set up at the vent clearing time with a negligible fraction of air in the region of the valve outlet and a relatively large fraction of air in front of the quencher outlet. To obtain a reference value for the actual degree of mixing during the expulsion of air, we shall estimate it for the example of GKM test 252 (Figure 3.3).

Since the water slug must first be expelled, after the valve opens the pressure in the blowdown pipe of the GKM test stand

rises (except for very long valve-opening times or very high condensation rates) to a value which is higher than the value in the steady state. As soon as the water slug is expelled, the exhaust velocity increases within a few milliseconds from the final water velocity to the velocity of sound.

It is demonstrated in /2/ that the volume increase of the bubble required for this occurs within a correspondingly short time. Then the pressure in the pipe drops to the steady-state final value. Thus, the maximum in the pressure variation of the transducer P_{DE} before the nozzle inlet practically coincides with the beginning of air expulsion; see Figure 3.3.

When the air bubbles are formed, water is displaced because of the internal pressure. As this happens, the many small bubbles forming at the outlet openings of the perforated-pipe quencher coalesce into larger units. As soon as the combined size of all bubbles is comparable to the tank diameter, the bubble internal pressure fully loads the bottom because of the comparatively small lateral extension of the test tank (Figure 4.1), i.e., there is a uniform spreading of the pressure in the test stand. Consequently, the bubble pressure can be measured by the pressure transducers at the bottom of the tank. At the time of the first pressure maximum of a pressure curve thought of as being smoothed, the bubble is growing so rapidly that the afterflowing air causes a constant bubble pressure. We may therefore assume that the air expulsion lasts

beyond this time. Thus, the time of [redacted] ms entered in Figure 3.3 represents a lower estimate of the air expulsion time.

Approximately [redacted] kg of mixture can flow out during this time.+) In comparison to this expelled quantity, about [redacted] kg of air is present at the beginning of the test. Therefore, at least [redacted] parts of steam are admixed with one part of air during the air expulsion. For comparison, about [redacted] parts of steam would be admixed with one part of air for homogeneous mixing at the vent clearing time with a pressure of [redacted] kg/cm^2. Thus, the lower estimate made here indicates a very good mixing of steam and air at the clearing time. The realistic estimate of [redacted] ms for the expulsion time is also entered in Figure 3.3. There is a nearly homogeneous mixing for that time.

3.3 Pressure drop during mixture expulsion

The steam-air mixture is expelled in the test stand through approximately [redacted] bores. The number of bores in the plant is increased in proportion to the flow rate and is approximately [redacted]. The boundary area available for condensation between the forming bubbles and the water is larger by an order of magnitude with the perforated-pipe quencher than with the plain-ended pipe, where the mixture is expelled as a compact

---

+) In comparison, [redacted] kg/s of steam flows out during steady-state operation with a lower initial pressure.

unit. Because of this intensive contact, the steam fraction contained in the mixture can condense out spontaneously. In addition, the air is then cooled down. As the high-pressure mixture of steam and air flows out, three mechanisms act to produce a distinct decrease of the pressure:

- The outflowing mixture is accelerated to the speed of sound and the pressure is thereby reduced to the critical value. The dynamic pressure component is throttled outside the nozzle by a Carnot transition. Therefore, only a slight pressure recovery occurs.

- The steam precipitates from the mixture by spontaneous condensation. There remains only the steam fraction which corresponds to the saturation content of the air. Associated with this is a pressure drop to approximately the partial pressure of the air.

- Finally, the air is cooled down from saturated-steam temperature to approximately the pool temperature. An additional pressure drop is associated with this.

The influence of condensation on the pressure drop clearly outweighs the other two components. Therefore, the process of spontaneous condensation shall be examined in somewhat more detail. For that purpose we use a momentum analysis for the oscillation process.

If we start out from the plane model which holds in the test

stand[+)], then for the air layer illustrated in Figure 3.4 in the equilibrium state it follows that the pressure in the air bubble is equal to the hydrostatic pressure

$$p_g = p_0 + \varrho H g$$

An overpressure or underpressure relative to this equilibrium pressure accelerates the water layer:

$$p - p_g = -\varrho H b$$

Integration of the pressure variation with respect to time from the passage through the equilibrium pressure τ_g to the pressure maximum τ_{max} leads to:

$$\int_{\tau_g}^{\tau_{max}} (p - p_g)\, dt = -\varrho H \int_{\tau_g}^{\tau_{max}} b\, dt$$

$$= -\varrho H w_{max}$$

If we neglect damping, then the areas F_1 and F_2 in Figure 3.4 must be equal when the air oscillation is developed, since in both cases the impulse corresponding to these areas accelerates the water mass above the air layer to the maximum velocity.

If now the condensation is spontaneous and complete when the steam-air mixture is expelled, i.e., if the water pool sees only the expelled air, then the kinetic energy of the oscillation

---

[+)] See also the illustrations in Sections 4.2.4 and 4.2.5.

can have been brought into the oscillatory system only by this air and the previously expelled water. Then, if we neglect damping and remember that the steam has surely condensed out by the time the oscillation has developed /3/, the area F_0 must also be equal to F_1 or F_2. In this regard it should also be pointed out that the impulse area F_0 originates only to a small extent from the water expulsion prior to the vent clearing time and is generated primarily by the air expulsion, as can be seen without difficulty from Figure 3.3.

Table 3.1 contains evaluations of impulse areas for tests with small volumes of air. The results are plotted in Figure 3.5 without dimensions. From the first to the third half-oscillations, the impulse areas decrease practically linearly in all cases. This is a manifestation of the damping produced by friction. If we assume that an appreciable amount of residual steam condenses out only during the first undershoot, then the area $2F_1$ would be enlarged by this, i.e., the oscillation would be stimulated. Now, we may assume /3/ that at a still later time the steam has surely condensed out. But the fact that the impulse areas $2F_1$ to $2F_3$ decrease linearly indicates that such a stimulation of the oscillation does not occur, i.e., that at the time of the first undershoot no appreciable amount of steam condenses out any longer. We may therefore assume that the steam has condensed out nearly spontaneously and completely.

It is also noteworthy in Figure 3.5 that the decrease of the impulse areas from F_0 to F_1 can differ distinctly for different tests with the same test parameters. The damping in the initial phase, during which the many individual bubbles coalesce into larger units and coupled oscillations occur, obviously varies and depends on random events. This might be the reason for the relatively large scatter of the measurement values illustrated in more detail in Section 4.

4. Vent clearing tests and discussion of results

In the condensation test stand in the Mannheim Central Power Station (GKM), very extensive tests were performed with the HS 1 quencher in order to investigate the influence of parameter variations on the bottom pressures during vent clearing and to find a favorable combination of parameters for the plant. All the GKM tests and also supplementary tests in the model test facility in Grosswelzheim (Gwh) to determine the influence of the free water area were considered in the evaluation.

4.1 Description of the test set-up in the GKM

Figure 4.1 shows the test set-up of the model quencher in the GKM test stand for [redacted] different air volumes. The most important measurement points in the blowdown pipe and on the tank bottom are shown.

Figure 4.2 presents a comparison of two quencher configurations in the tank with approximately equal air volumes but different lengths of blowdown pipe. It should be noted that the high quencher is provided with a central double pipe. Differences with respect to the single pipe occur only if the central pipe is submerged into the water at the beginning of the test. For the tests with the central pipe not submerged, which are the only ones used in this report, a comparison of the pressure build-up in the blowdown pipe with other arrangements is presented in Figure 4.3. There is practically no difference.

Because of the larger distance of the quencher from the bottom with a double pipe, the test stand is equipped with special instrumentation to measure the pressures below the quencher at a distance which corresponds to the bottom distance in the tests with a single pipe. But the pressures at the more distant bottom are also recorded for comparison.

At the test scale used in the GKM, the rated steam-flow density is reached when saturated steam appears before the full-size valve at only about [redacted] kg/cm^2 (absolute). During the vent clearing in most of the tests, a transient pressure occurred in the pipe which limited the flow-rate toward the end of the process. For transposition to the plant, a computational correction is performed for this phenomenon in the manner illustrated in the Appendix.

The model quencher corresponding to the full-size version (Figure 2.2) is shown in Figure 4.4. The various hole-array patterns are illustrated in Figure 4.5; variants [redacted] were utilized only in the preliminary tests.

4.2 Dependence of the bottom pressure on individual parameters

Table 4.1 contains a chronological list of all vent clearing tests in the GKM with the HS 1 quencher and the measurement values obtained in them. The quantities exerting an influence on the clearing process are discussed individually in the following:

4.2.1 Influence of the exhaust area

At the beginning of the GKM test series with the HS 1 model quencher, tests were performed on the hole layout. The various hole-array patterns are compiled in Figure 4.5. The variation extends over the total area installed and also over the inclination of the hole arrays. The results of these tests are illustrated in Figure 4.6. Measurement points for constant exhaust area but different hole-array pattern or inclination (versions 1 and 3, on the one hand, and versions 2 and 4, on the other hand; see also Figure 4.5) are classified in each instance in a common scatter-band with the same maximum percentage deviation from the mean values. Thus, an influence is exerted only by the exhaust area and not by the hole-array inclination. A smaller quencher exhaust area also leads to lower bottom pressures if the other parameters are unaltered.

The amount of air expelled per unit time depends on the exhaust velocity, the partial pressure and the exhaust area. As is shown later in Section 4.2.6, the first two parameters do not vary. Therefore, a decrease of the exhaust area leads to a prolongation of the expulsion time for the enclosed amount of air. Thus, it can also be seen from Figure 4.6 that the bottom pressures become lower with longer expulsion time. The ratio of air volume to this exhaust area V_{total}/F_D, which characterizes the expulsion time, is transposed to the plant approximately unaltered.

All other tests with the HS 1 quencher were performed with hole-array pattern 4.

4.2.2 Influence of the valve-opening time

The influence of the valve-opening time can be determined from several groups of tests with equal submergence and equal volume and with otherwise unaltered parameters. Whereas no dependence of the bottom pressures on the valve-opening time can be found for a submergence of [redacted]m (Figure 4.7), the pressure amplitudes decrease clearly with longer valve-opening time for a submergence of [redacted]m (Figure 4.8). At [redacted] m submergence, the pressure amplitudes are again found to be independent of the opening time (Figure 4.9). Air-volume changes only cause changes in the magnitude of the pressure amplitudes, but do not affect the trend of the dependence on the opening time. No unambiguous overall influence of the valve-opening time on the bottom pressure can be observed.

4.2.3 Influence of the submergence

The maximum pressure amplitudes at the bottom for a constant valve-opening time of [redacted]ms are plotted versus the submergence in Figure 4.10. For submergences of [redacted]m, the measured values are at approximately the same level. For a submergence of [redacted]m, they are distinctly lower for approximately the same air volume.

4.2.4 Influence of the air volume

When the air is expelled, the water above the quencher is forced into motion in the direction of the water surface, whereas a transverse motion is prevented by the tank wall. The air bubbles emerging at the individual holes are distributed over a large portion of the tank's cross-section. Under this assumption, the air oscillations during vent clearing in the GKM tank can be treated as a two-dimensional problem.

According to Section 3.3, the impulse of the moving water mass derives primarily from the expelled air volume. For constant tank cross-section, the impulse to the moving water mass is proportional to the thickness of the air layer, which is thought of as being uniformly distributed. In turn, the impulse of the water mass is a measure for the pressure at the bottom of the tank. Since the cross-sectional area is equally large for all tests in the GKM tank, the thickness of the air layer is proportional to the expelled volume of air. Thus, an increase of the expelled volume of air results in an increase of the bottom pressure, as is confirmed by the GKM tests (4.11). Of course, it should be noted here that a change of the air volume involves a change of the expulsion time. Thus, the variation of another parameter is contained implicitly in Figure 4.11.

4.2.5 Influence of the free water-area

In the GKM test tank the dependence of the bottom pressure on the air-layer height could be obtained only by varying the air volume, whereby the air expulsion time was also necessarily varied. For constant air volume and thus constant expulsion time, the air-layer height can be varied by varying the cross-sectional area of the tank. We thus obtain the dependence of bottom pressure on tank size.

Supplementary vent clearing tests were performed in the Grosswelzheim model test stand in order to be able to record this influence of the free water-area. Figure 4.12 shows a perspective view of the test arrangement in the model tank. A cross-shaped perforated-pipe quencher was used as the blowdown geometry. The submergence was [redacted] m with a distance of [redacted] m from the cross-shaped quencher to the bottom. To limit the free water area, a cylindrical pipe was placed around the blowdown pipe with the cross-shaped quencher. It projected above the water surface, so that a coupling between the internal and external water spaces was prevented (Figure 4.13). A piezoelectric pressure trandsucer, which recorded the pressures during vent clearing, was mounted below the cross-shaped quencher on the bottom of the model tank.

The throttle nozzle after the valve was used to adjust the maximum mass flow density, which was set at [redacted] kg/m^2s for this test. Since the rapidity of the pressure build-up in the

relief pipe is determined by the time variation of the mass flow through the throttle nozzle, the determinative factor is no longer the mechanical opening time of the valve, but rather the pressure rise time before the nozzle. Therefore, this pressure rise time before the nozzle was defined as the "fictitious" valve-opening time $\tau_{\ddot{o}}$.

Since the surface area of the blowdown pipe in the model test stand is very large compared to the inflowing amount of steam, the blowdonw pipe was heated electrically between the valve and the model tank (wall temperature approximately [redacted] C at beginning of test) in order that the tests not be falsified by too high condensation rates.

The test results are illustrated in Figure 4.14 for a valve-opening time of approximately [redacted] ms. We recognize a distinct decrease of the maximum pressure amplitudes at the bottom as the free water area increases.

We also ran tests in which the quencher had an eccentric position in the restricted water space (see Figure 4.13). But these measurements showed no difference in comparison with the central configuration, as is also evident from Figure 4.14.

As was already stated in Section 4.2.4, the water column above the expelled air layer can only move in the vertical direction. The air oscillations following vent clearing in a narrow tank can be treated mathematically as a two-dimensional oscillation problem:

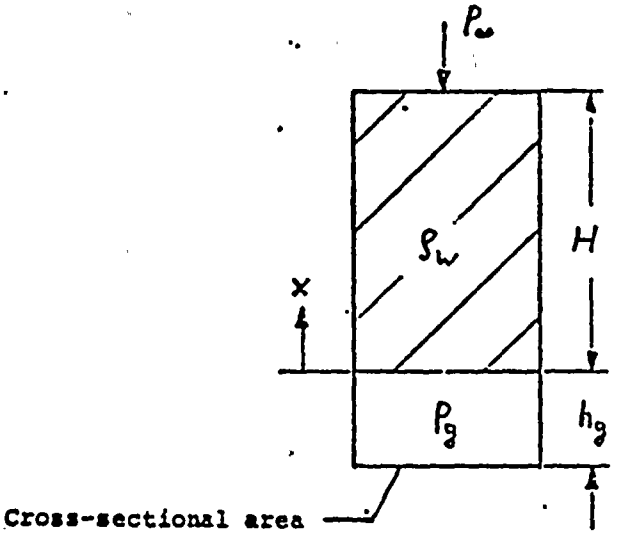

Subscript g:
equilibrium state

The equation of motion for the water mass reads:

$$\ddot{x} + g - (\rho - \rho_\infty) \cdot \frac{F_w}{m_w} \qquad (1)$$

with

$$\rho = \rho_g \left(\frac{V_g}{V}\right)^\kappa = \rho_g \left(\frac{h_g}{h_g + x}\right)^\kappa \qquad (2)$$

and

$$\frac{m_w}{F_w} = \rho_w \cdot H \qquad (3)$$

Therefore:

$$\ddot{x} - \frac{p_g}{\rho_w \cdot H} \cdot \left(\frac{h_g}{h_g + x}\right)^{\kappa} + \frac{p_\infty}{\rho_w \cdot H} + g = 0$$

For $|x| << h_g$, we obtain as an approximation:

$$\ddot{x} + \frac{\kappa \cdot p_g}{\rho_w \cdot h_g \cdot H} \cdot x = 0$$

If we assume sinusoidal oscillations for small deflections:

$$x = x_{max} \cdot \sin \omega t,$$

then the natural frequency of the system is given by

$$\omega = \sqrt{\frac{\kappa \cdot p_g}{\rho_w \cdot h_g \cdot H}}$$

The oscillation period is thus calculated as

$$\tau_s = 2 \cdot \pi \cdot \sqrt{\frac{\rho_w \cdot h_g \cdot H}{\kappa \cdot p_g}}$$

The following quantities are constant for all the tests:

$\rho_w = 10^3$ kg/m^3

H = [redacted] m

κ = [redacted]

p_g = [redacted] kg/cm^2

V_g = [redacted] m^3

Using this data, the oscillation period was calculated as a function of the free water-area F_W in Figure 4.15. The

calculation always yields a smaller value compared to the oscillation period measured in the model tank. This can be explained by the fact that the air does not fill up the entire cross-sectional area uniformly and thus the actual air-layer thickness is larger than calculated. According to Eq. (7), this leads to a larger oscillation period. The oscillation period measured in the experiment can therefore only be equal to or greater than the calculated one. As is also evident from Figure 4.15, the relative deviation of the measured oscillation period from the calculated oscillation period increases with increasing water area, as should also be expected.

4.2.6 Influence of the vent clearing pressure

During the test series with the HS 1 quencher, we attempted to achieve short opening times, despite low control pressures, by making changes in the valve. In three consecutive tests there was an abnormal opening behavior of the valve, which was able to be confirmed subsequently. Although these tests were run in an irregular manner, they provide important information concerning the influence of the vent clearing pressure on the bottom pressures.

Figures 4.16 and 4.17 show measurement traces from two of the mentioned tests. The peculiarity is that approximately [redacted] s before the actual opening, the valve has lifted slightly for about [redacted]s and some steam has passed into the blowdown pipe. As a result, the pressure in the blowdown pipe rises and the water level is forced down. But no air emerges, as shown by

the non-responding bottom pressure transducers. The valve now opens in this condition. For comparison, Figure 4.18 shows the measurement trace of a "normal" test with otherwise identical test parameters. From the compilation of measurement values in Table 4.2 we can see that the vent clearing times are clearly smaller in the two "pre-impinged" tests than in the comparison tests, and the vent clearing pressures are only about [redacted] of the comparison value. Nevertheless, bottom pressures result which are necessarily included in the scatter band of the "normal" tests (circled stars in Figure 4.8). This test result demonstrates that, at the very least, the vent clearing pressure can have no major influence on the bottom pressures.

To better evaluate the influence of vent clearing pressure, the measured bottom pressures are plotted versus the vent clearing pressure in Figures 4.19 to 4.23 for tests with identical test parameters (quencher exhaust area, air volume, submergence).+) The vent clearing pressure was defined here as the maximum reading of the pressure P_{DE} before the quencher at the vent clearing time. To some extent, the measurement points form a wide scatter band, which indicates that the vent clearing pressure is not a significant parameter. No clear dependence of the bottom pressure on the vent clearing pressure is discernible.

+) A compilation of the measurement values can be found in Table 4.3.

This distinguishes the perforated-pipe quencher from the plain-ended pipe, where a very clear dependence exists.

In order to be able to recognize the influence of the vent clearing pressure on the pressure oscillations at the bottom independently of other influential parameters, it is assumed that in the cases considered here the degree of mixing is always the same. In other words, the mean air partial pressure during the expulsion of the steam-air mixture is in a fixed ratio to the air partial pressure for the limiting case of homogeneous mixing. Moreover, we assume saturated-steam conditions, which is surely approximately correct.

Only an indirect influence of the vent clearing pressure is conceivable. For a higher vent-clearing pressure, a larger amount of steam is expelled with the air. It was shown in Section 3.3 that at the maximum possible vent clearing pressure

of [redacted] kg/cm^2 (gauge) in the GKM test stand, no clear contribution of the steam to the air oscillations can be observed. Thus, the problem reduces to the question as to whether the maximum possible amount of steam corresponding to the maximum vent clearing pressure in the plant can also condense out of the steam-air mixture so quickly that the steam continues to supply no appreciable contribution to the air oscillations. This problem is discussed in Section 4.3.

4.2.7 Influence of the air temperature in the pipe

Before beginning a vent clearing test, cold water was sprayed in for several minutes just below the valve in order to cool down the blowdown pipe, which was usually still hot from the preceding test, to approximately 30-35° C. Then there was a flush with air, which then also assumed this temperature. In order to examine the influence of air temperature on the bottom pressures, the flushing in Test 254 was performed with air but not with water. The blowdown pipe and the air enclosed in it were at a temperature of about [redacted] C at the beginning of the test.

As is shown by the compilation of values in Table 4.4, the condensation rate at the pipe wall is lower for the hot pipe and consequently the vent clearing is higher then in comparable tests with a cold pipe, but the bottom pressures are clearly lower. As is shown in Table 4.4, the air partial pressure P_L for the case of homogeneous mixing in Test 254 is

clearly lower than in the comparison tests.

Thus, both the volume of air expelled and also (because of the lower partial pressure) the amount of air expelled per unit time are lower. Both effects tend to produce lower bottom-pressures, as was described in Sections 4.2.1 and 4.2.4.

In order to exclude the influence of air temperature, we conservatively use only tests with a cold blowdown pipe when making statements concerning the bottom load in the suppression chamber. It should also be mentioned that an air partial pressure of [redacted] kg/cm^2 (absolute) results in the plant for homogeneous mixing at the vent clearing time with an initially cold pipe. This value nearly corresponds to the favorable value in the test stand for an initially hot pipe.

4.2.8 Influence of an overpressure in the blowdown pipe

In loss-of-coolant accidents we can conceive of operating conditions in which an overpressure appears in the blowdown pipe relative to the suppression chamber via the snifting valves, and the water level in the pipe has dropped.

Tests were performed in the GKM with an overpressure of [redacted] kg/cm^2 in the pipe and a submergence of [redacted] m. The air volume in the pipe due to the lowering of the water level by [redacted] m is then [redacted] m^3. If we convert the amount of air enclosed in this volume with the pressure ratio, we obtain an air volume of [redacted] m^3 at [redacted] kg/cm^2 (absolute).

The maximum measured pressure amplitudes are entered in the Table below for tests with and without an overpressure in the pipe. The only essential difference in the test parameters is in the air volumes.

Test No.	V^*_L	Initial pressure in the pipe	Pressure amplitudes at the bottom
	m^3	kg/cm^2 (absolute)	kg/cm^2
[redacted]			

*relative to 1 kg/cm^2 (abs.)

As shown in the Table, the magnitude of the pressure amplitudes with elevated internal pressure in the pipe is attributable to the influence of the expelled volume of air. The scatter band for all comparable tests can be found from Tables 4.1 and 4.5 and Figure 4.24.

4.2.9 Influence of an elevated pressure in the tank

The tests in the GKM with elevated pressure in the tank are listed separately in Table 4.5. [redacted]. It should also be mentioned that in Figure 4.24 only the pure air-oscillations are plotted and not high-frequency pressure peak values during air expulsion. Because of an amplification effect related to the test stand, the latter are greater at the bottom of the tank than at the

struts (see test set-up Figure 4.2). Therefore, the values at the bottom sometimes exceed the maximum values of the air oscillations.

4.2.10 Influence of water temperature

As is made clear by Figure 4.25, the bottom pressure rises with increased pool temperature. Simultaneously the oscillation period also becomes greater (Figure 4.26).

From the varying oscillation period we can infer that higher water temperatures are coupled to a larger oscillating volume of gas. The relation between gas volume and oscillation period is described, for example, in /2/ (see also Section 4.2.5).

The longer oscillation period is explained first by the fact that in a warmer pool the air is cooled down less intensely and therefore occupies a larger volume. Secondly, we may assume that a residual amount of steam, corresponding to the saturation steam content associated with the air temperature, always remains in the air. The steam content is negligible for lower air temperature, but provides a significant contribution for higher temperatures (Figures 4.27).

This noncondensing steam content must be added to the quantity of air. Thus, more "effective gas" flows out in the same time for higher water temperatures, resulting in increased bottom pressures. But as shown in Figure 4.25, the effect is not large.

The oscillation period calculated according to the two-dimensional model (Section 4.2.5) when the steam content is taken into consideration is entered in Figure 4.26. It was assumed here that the air saturated with steam has assumed the pool temperature.

4.3 Concise evaluation of the measurement results

In examining the dependence of the bottom pressure, the following parameters were found to have no influence:

- Submergence in the range of about [illegible]m under consideration
- Length of the blowdown pipe
- [illegible]

In contrast, the following parameters exert a substantial influence on the pressure amplitudes:

- Quencher exhaust area
- Amount of air in the blowdown pipe
- Free water-area
- Pool temperature.

The bottom pressures increase with increasing quencher exhaust area, increasing amount of air in the blowdown pipe, decreasing free water-area and increasing pool temperature.

In contrast to the plain-ended pipe, the following were found to be nonsignificant parameters for the perforated-pipe quencher:

- Valve-opening time
- Vent clearing pressure.

Of course, these two quantities may be considered as a unit, since the valve-opening time affects primarily the pressure variation in the pipe.

According to the discussion in Section 4.2.6, the pressure of the steam-air mixture at the vent clearing time has no direct influence. Rather, the important question is whether in practically occurring cases the amount of steam included with the air and increasing with the vent clearing pressure can condense out of the expelled mixture so quickly that there is no substantial contribution of the steam to the air oscillations. From this discussion, the amount of steam expelled with the air is found to be another possible quantity exerting an influence on the pressure amplitudes at the bottom.

The amount of steam that can condense in a given time depends on the heat transfer at the boundary between the steam-air mixture and the water, which in turn depends on the temperature difference between the two materials for otherwise constant conditions. Since the pressure of saturated steam increases very rapidly with temperature (as made clear in Figure 4.28), it follows that the temperature difference relative to the water is always very large and therefore the heat transfer is good as long as a high partial pressure of the steam prevails in the expelled mixture. Thus, the major

portion of the steam condenses out very quickly, independently of the amount. Therefore, the influence on the oscillation process is limited in any case to the amount of residual steam and thus is substantially independent of the total amount of steam admixed with the air.

The vent clearing tests at high pool-temperature give a clear indication as to how well this residual amount of steam condenses out (Section 4.2.10). The increase of the bottom pressures measured there can be attributed to the amount of steam remaining in the air, which corresponds to the saturation state of the air and therefore does not condense out anyway. A stimulation of the oscillation, which is attributable to a slower condensation of the amount of steam contained in addition to that, cannot be detected from the measurements. Thus, the condensation occurs in hot water just as well as in cold water, although in hot water the heat is transferred distinctly more poorly because of the smaller temperature drop between the portion bounding the air bubbles and the rest of the pool. Accordingly, we can assume that the amount of steam admixed with this air provides only a small contribution, negligible in first approximation, to the air oscillations. Because of this, the influence of the vent clearing pressure on the oscillations can also be neglected in first approximation.

5. Expected dynamic pressure load in the suppression chamber

In the preceding Section 4 we considered all the GKM tests with the model quencher HS 1 in order to demonstrate the effects of parameter variations. The nozzle with the fourth variant of the hole-array size and with the small volume of air is used as a reference quencher to transpose the measurement values to the plant (second test series with NW△▽ blowdown pipe and third test series with high quencher). The large-scale version of the quencher in the power plant was matched to this reference quencher with respect to the operationally relevant parameters.

5.1 Comparison of parameters in the test stand and plant

In Table 5.1 the parameters of the test stand and plant are compared to each other and the transposition factors are indicated. Agreement exists for the following quantities:

- geometrical similarity of the quencher;
- characteristic dimensions of the quencher hole array;
- steam flow density for steady-state condensation;
- vertical dimensions (submergence; length of the blowdown pipe is within the range of parameters that was found to have no influence when varied);
- ratio of the air volume in the relief system to the quencher's cross-sectional area;
- ratio of the free water-area to the quencher's cross-sectional area;

- ratio of the total volume in the relief system at the vent clearing time to the total aperture area of the quencher.

Differences are found with respect to the following parameters:

- absolute magnitude of the air volume;
- absolute size of the quencher;
- absolute size of the tank;
- absolute exhaust area of the quencher;
- vent clearing pressure.

The total amount of energy brought in increases with increasing air volume. Nevertheless, the air volume cannot be an absolute quantity of influence. Rather we are interested in knowing what mass of water this energy is distributed over and how quickly it is delivered. Therefore, the expelled air volume is to be expressed as a ratio to other quantities.

Table 5.1 shows that the horizontal dimensions of the power-plant quencher are increased by a factor of [redacted] relative to the model quencher (rows 9, 14 and 15 in Table 5.1). The quencher's cross-sectional area increases correspondingly by a factor of [redacted] (row 10). [redacted] (row 11). Thus, the larger volume of air is distributed over a mass of water enlarged laterally to the same extent. Since the air oscillations according to Section 4.2.5 represent practically a two-dimensional problem, no change occurs in the oscillation process and thus

also in the bottom pressures when we make the transposition from the model quencher to the large-scale version.

If we assume a free water-area enlarged in the same ratio as the quencher, then we obtain the cutaway section of the suppression chamber illustrated in Figure 5.1 in which the quencher is arranged somewhat eccentrically. According to the measurements described in Section 4.2.5, this eccentric configuration is of no significance. The radial boundary walls illustrated in Figure 5.1 are only fictitious and do not exist in reality. We may therefore assume that the air in the plant is somewhat more spread out proportionately than in the test plant, which leads to lower bottom-pressures. In addition, the oscillation then no longer occurs exclusively in the vertical direction.

The quencher exhaust area (row 22 in Table 5.1) was adapted to the flow rate (row 26) in order to achieve a constant mass flow density (row 27). On the other hand, according to the investigation in Section 4.2.1, the exhaust area has a clear influence on the bottom pressures, with a tendency for the pressure amplitudes to decrease for a prolonged expulsion time of the air, i.e., for a reduced exhaust area of the quencher. If we assume that the air distribution in the blowdown pipe at the beginning of the expulsion process, although not known exactly, is the same in the model and in the large-scale version and that the flush process is also the same,

than the air expulsion time is proportional to the ratio of the total volume of the relief system (row 6) to the quencher exhaust area (row 22). This ratio was also held nearly constant (row 23).

The vent clearing pressure (rows 29 and 30) still remains as a parameter which is not transposed as a constant. The presentation in Section 4.2.6 shows that the vent clearing pressure as such cannot be a relevant parameter with the perforated-pipe quencher, since the air from a given system always flows out at the same rate, independently of the vent clearing pressure. Only an indirect influence is conceivable, since for a higher vent-clearing pressure a larger amount of steam is expelled with the air. This additional steam must condense out quickly enough if it is to have no appreciable influence. These problems are discussed in more detail in Section 4.3. The investigations presented there make it clear that only a slight influence of the vent clearing pressure can be expected from this secondary effect. The influence of the vent clearing pressure on the pressure amplitudes at the bottom can be neglected in first approximation.

5.2 Transposition of measurement results to the plant

On the basis of the parameter comparison performed in the preceding Section, the measurement results in the GKM test stand for the KS 1 quencher with a total hole area of [redacted] cm^2 and an air volume of [redacted] or [redacted] m^3 can be transposed

directly to the plant as far as the air oscillations are concerned. The maximum values measured for a submergence of [redacted] are used for this transposition. The following three cases are to be distinguished:

Case	Designation	Maximum pressure amplitudes	
		positive	negative

KRAFTWERK UNION
AG PROPRIETARY INFORMATION

In the first two cases these expectation values might be exceeded by about [redacted] before they reach the desired maximum load of [redacted] kg/cm^2. In the third case, the exceedance limit is at [redacted].

Figure 5.2 also shows the pressure distribution for a simultaneous response of 3 relief valves and for coherent air oscillations. The distribution curves result with the assumptions explained in more detail in /4/. The maximum force on the bottom occurs for a uniform distribution of quenchers. The pressure acting on the average is then scarcely [redacted] of the peak value.

6. Transverse force on the quencher

To determine experimentally the transverse forces that occur during condensation, we used two linear displacement transducers (LVA) whose arrangement is shown in Figures 6.1 and 6.2. The measurement frame, which bears two inductive displacement transducers (LVA B and LVA C) separated by 90°, is secured in the tank by a diagonal brace. These displacement transducers make it possible to measure the deflection of the quencher and of the blowdown pipe and thus to determine the load acting at the quencher. The calibration curve applicable for both transducers is plotted in Figure 6.3.

The results of the transverse force evaluation for the GKM tests with the HS 1 perforated-pipe quencher (Tests No. 236 to 257) are compiled in Table 6.1. As the transverse force we used in each instance the resultant which resulted from the deflection of the blowdown pipe as measured by LVA B and LVA C at the most unfavorable time, i.e., the maximum value was determined. An unambiguous preferential direction of this force could be ascertained.

Since no clear dependence of the measurement results on the hole-array pattern, mass flow density, valve-opening time and submergence can be ascertained for the tests compiled in Table 6.1, the determination of the transverse force on the quencher in the plant was based on the maximum resultant load that

occurred during the tests. It was found to be [redacted] Mp in Test 243 I. The next-lower value was a load of [redacted] Mp in Test 261, i.e., about [redacted] less.

Under the assumption that the unsymmetry occurring in the test stand is not exceeded in the plant, the measurement value can be extrapolated to the maximum conceivable value in the plant, assuming a proportional dependence on the aperture area of the quencher and on the vent clearing pressure. With

n_F = [redacted]

and

n_p = [redacted]

we obtain

P = [redacted] Mp.

In addition, because of the hole arrays of [redacted] cm^2 on two arm ends, there is a thrust force which, for a vent clearing pressure of [redacted] kg/cm^2 (gauge) and taking into consideration the angle of [redacted] between the two arms, reaches a value of

S = [redacted] Mp.

Whereas the calculated thrust force corresponds to the actual maximum force occurring due to the unsymmetrical arrangement of the hole arrays on two arm ends, the values measured in the test stand are to be understood as the dynamic equivalent

load applicable for the test quencher. Figure 6.4 shows a measurement trace which makes it clear that the motion of the quencher builds up in pendulum form. The maximum deflection is therefore not the result of a constant acting force. It also contains the impulse from the preceding deflection to the opposite side, resulting in a dynamic load factor greater than 2. Accordingly, the force actually acting is smaller than half the measurement value. Therefore, the extrapolated value must also be reduced correspondingly in order to get the force that acts in a purely static manner. The maximum occurring transverse force (sum of thrust force and force from unsymmetry) does not exceed the specified value of [redacted]dp.

KRAFTWERK UNION AG PROPRIETARY INFORMATION

Table..... 2.1 - 6.1

6-46 - 6-74

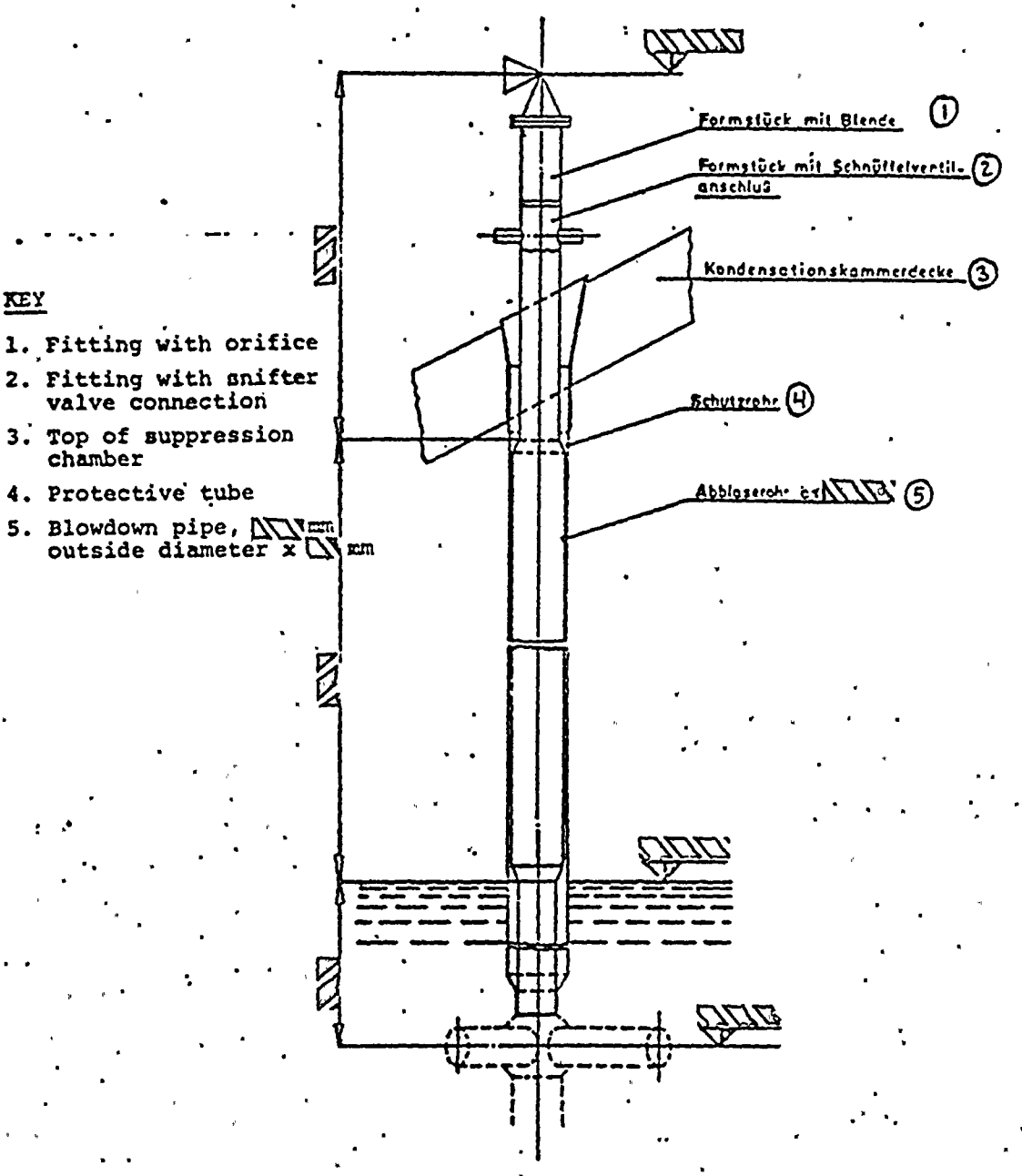

KEY

1. Fitting with orifice
2. Fitting with snifter valve connection
3. Top of suppression chamber
4. Protective tube
5. Blowdown pipe, mm outside diameter x mm

Bild 2.1 Figure 2.1

KKB - Anordnung und Ausführung des Abblaserohres

KKB - Configuration and construction of the blowdown pipe

KRAFTWERK UNION AG PROPRIETARY INFORMATION

Figure..... 2.2

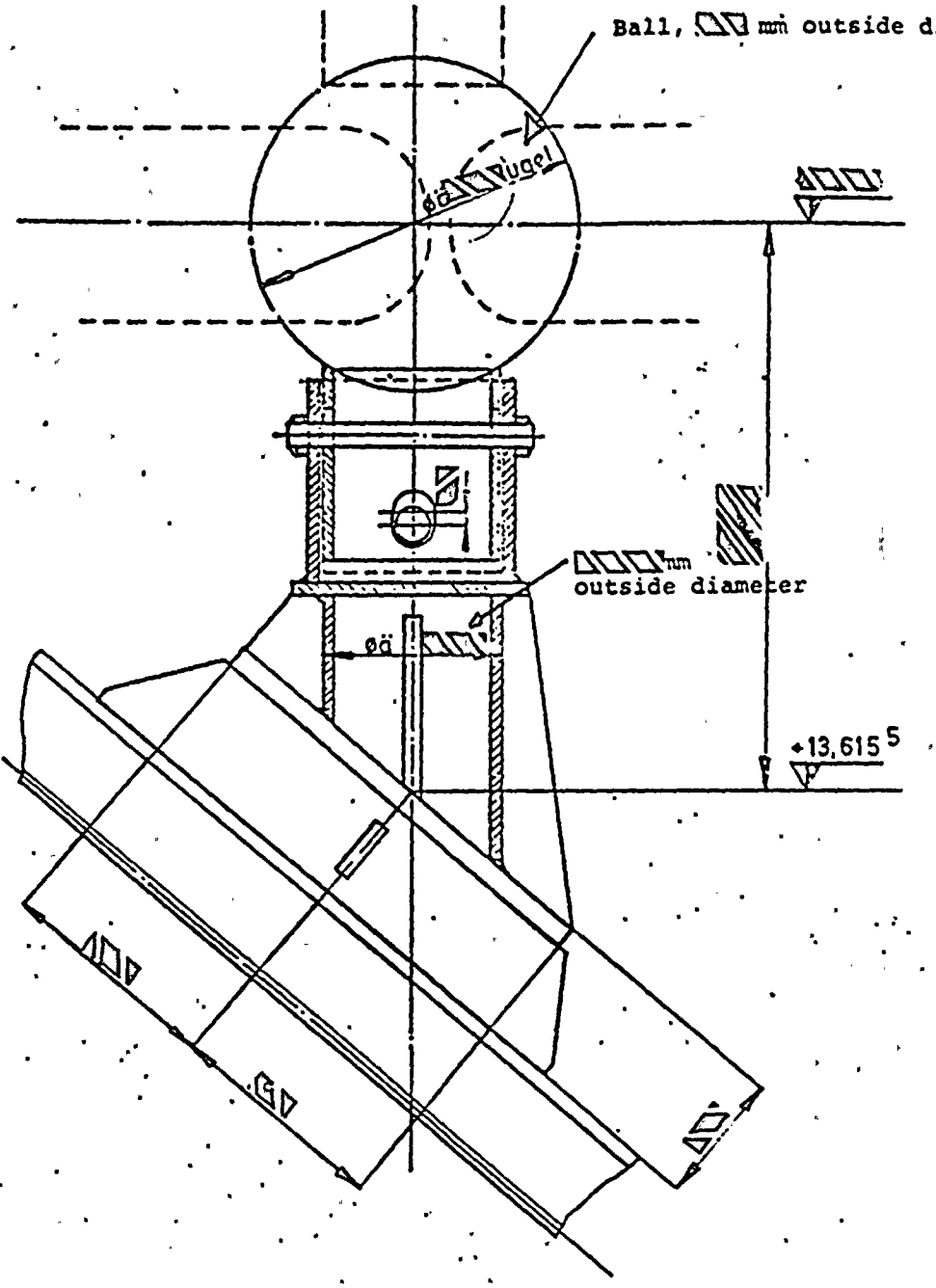

Bild 2.3 Figure 2.3

KKB - Bodenverankerung der Lochrohrdüse

KKB - Bottom bracing of the perforated-pipe quencher

KRAFTWERK UNION AG PROPRIETARY INFORMATION

Figure..... 3.1 - 3.3

6-78 - 6-80

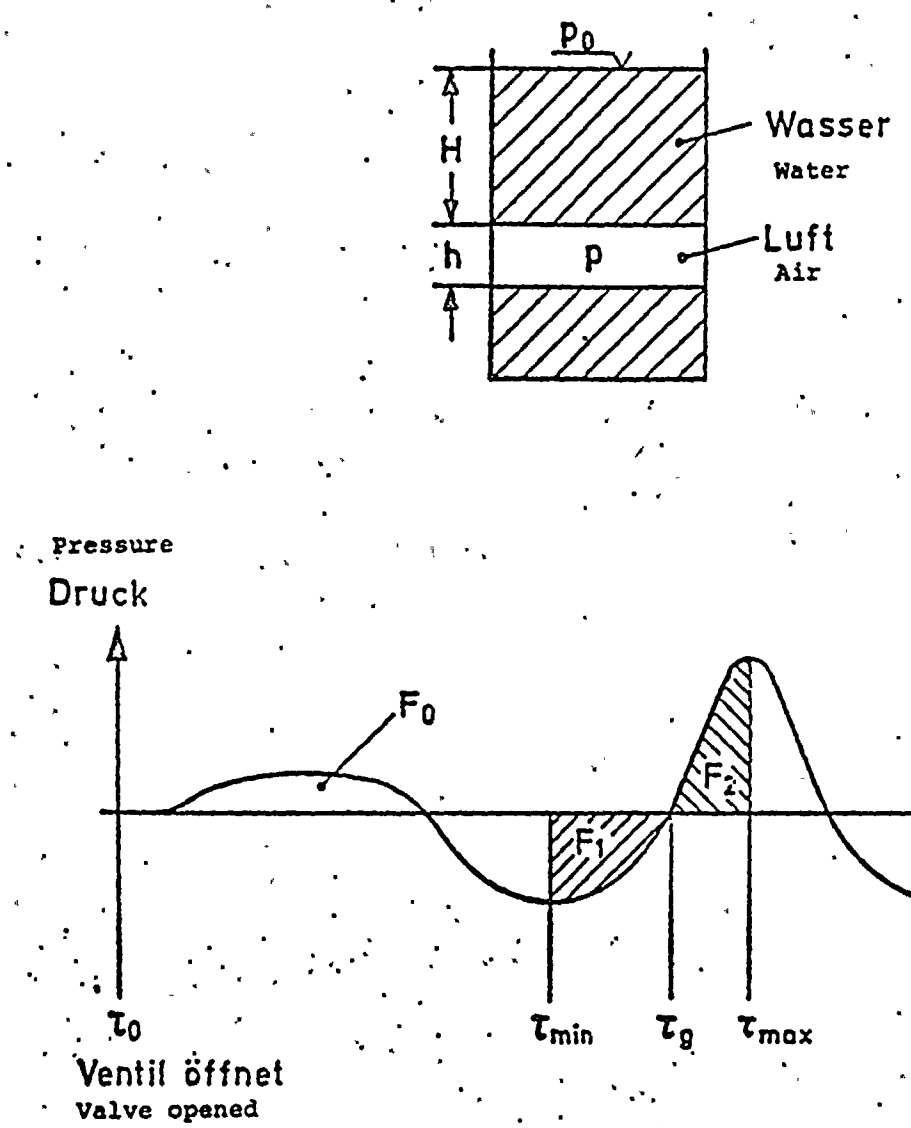

Bild 3.4 Figure 3.4

Impulsflächen bei den Luftschwingungen Prinzipskizze, Dämpfung vernachlässigt

Impulse areas for air oscillations. Basic sketch, damping neglected

KRAFTWERK UNION AG PROPRIETARY INFORMATION

Figure..... 3.5

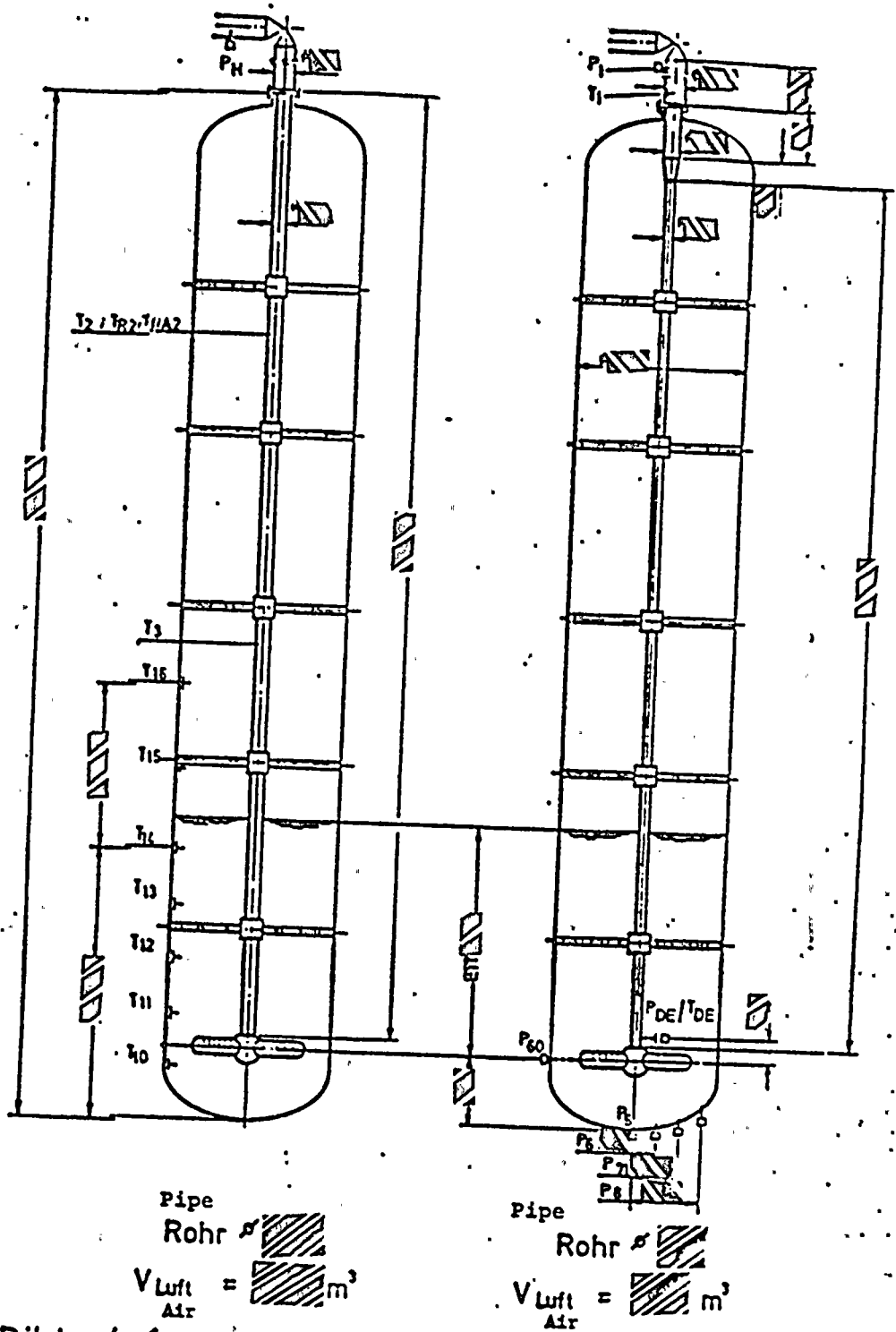

Bild 4.1 Figure 4.1

Anordnung der Lochrohrdüse HS1 im GKM-Versuchsstand
Variation des Luftvolumens

Arrangement of the porforatod-pipe quencher HS1 in the GKM test stand
Variation of the air volume

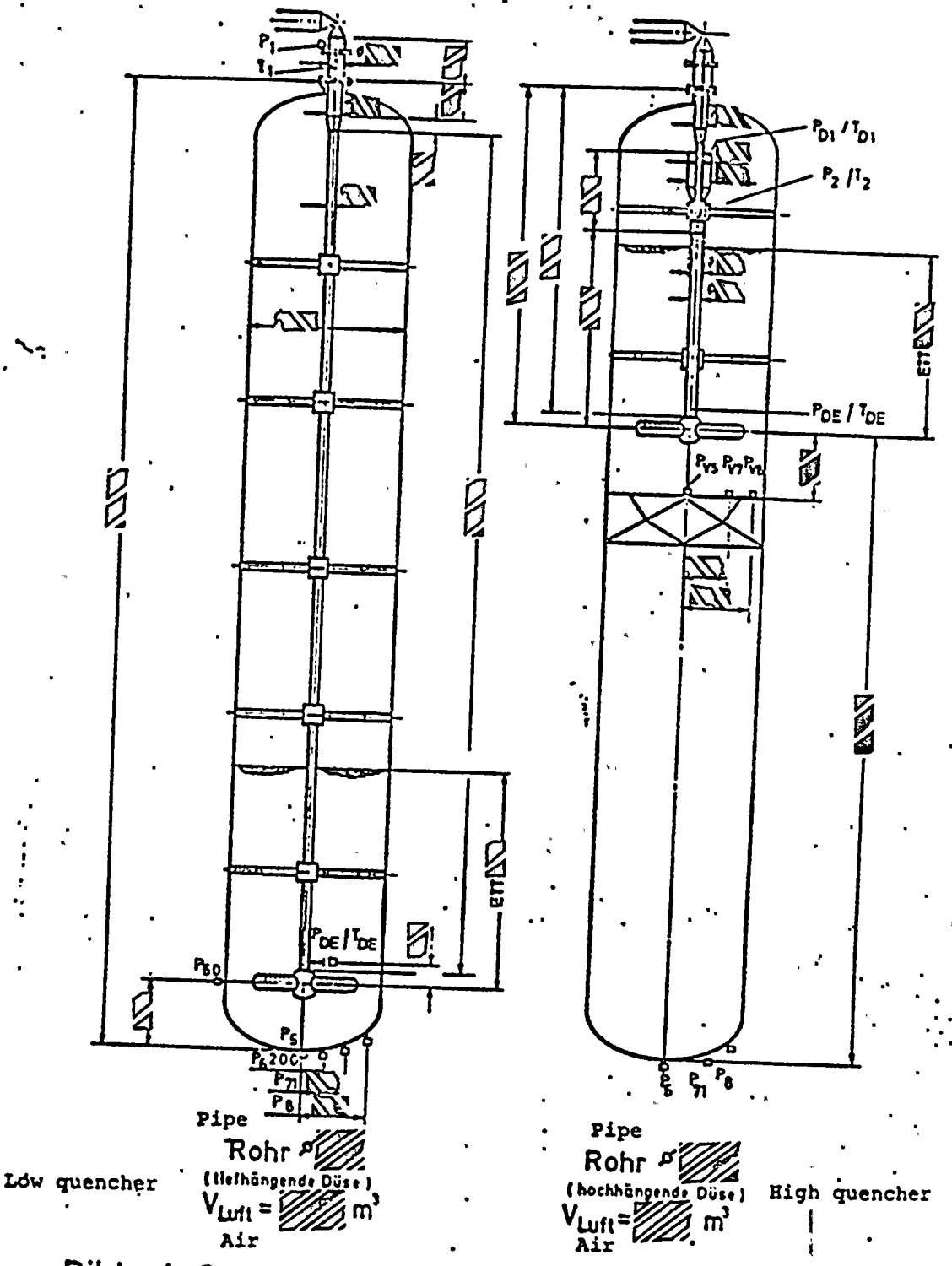

Bild 4.2 Figure 4.2

Anordnung der Lochrohrdüse HS 1 im GKM-Versuchsstand

Tief- und hochhängende Düse

Arrangement of the perforated-pipe quencher HS1 in the GKM test stand
Low and high quenchers

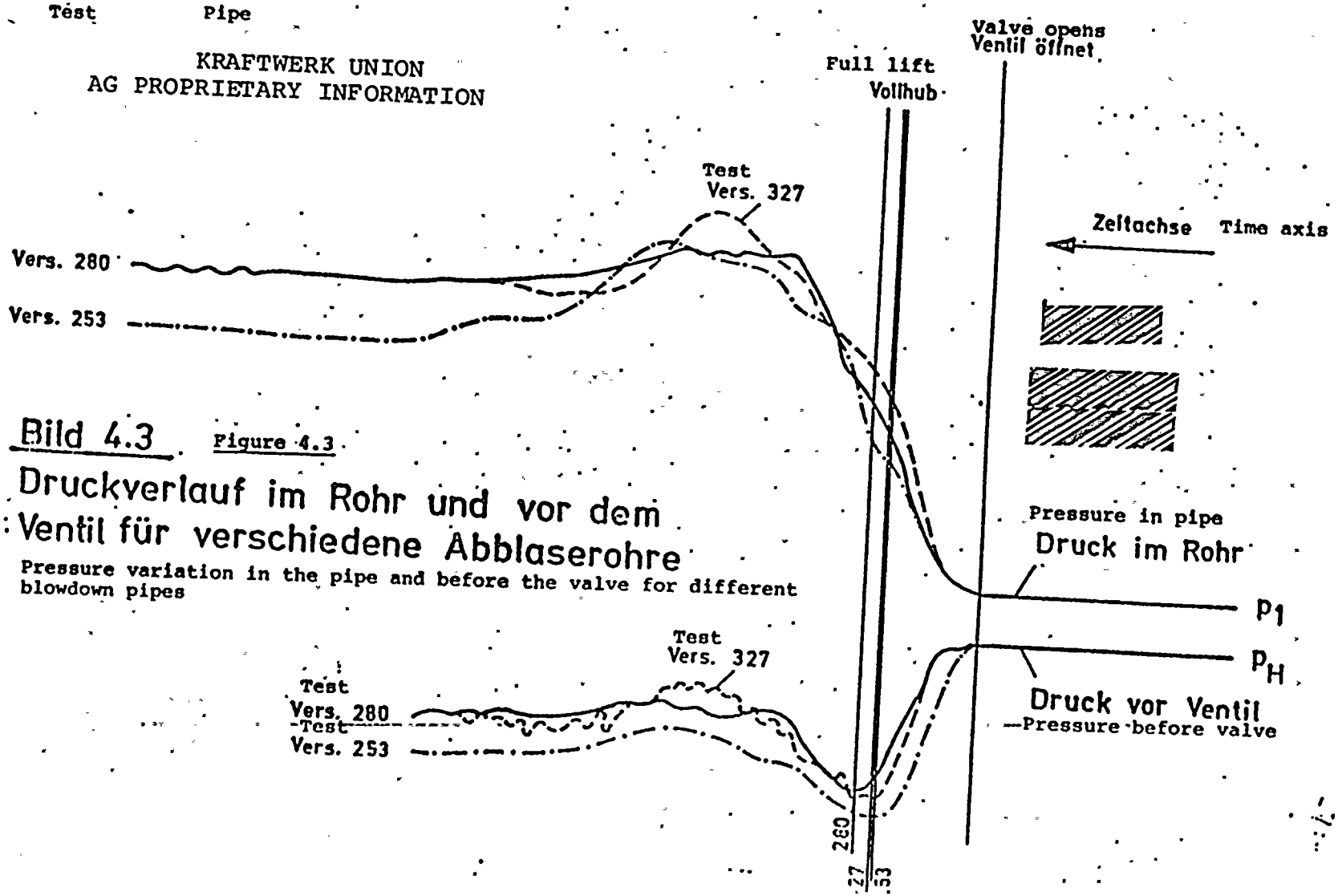

Bild 4.3 Figure 4.3

Druckverlauf im Rohr und vor dem Ventil für verschiedene Abblaserohre

Pressure variation in the pipe and before the valve for different blowdown pipes

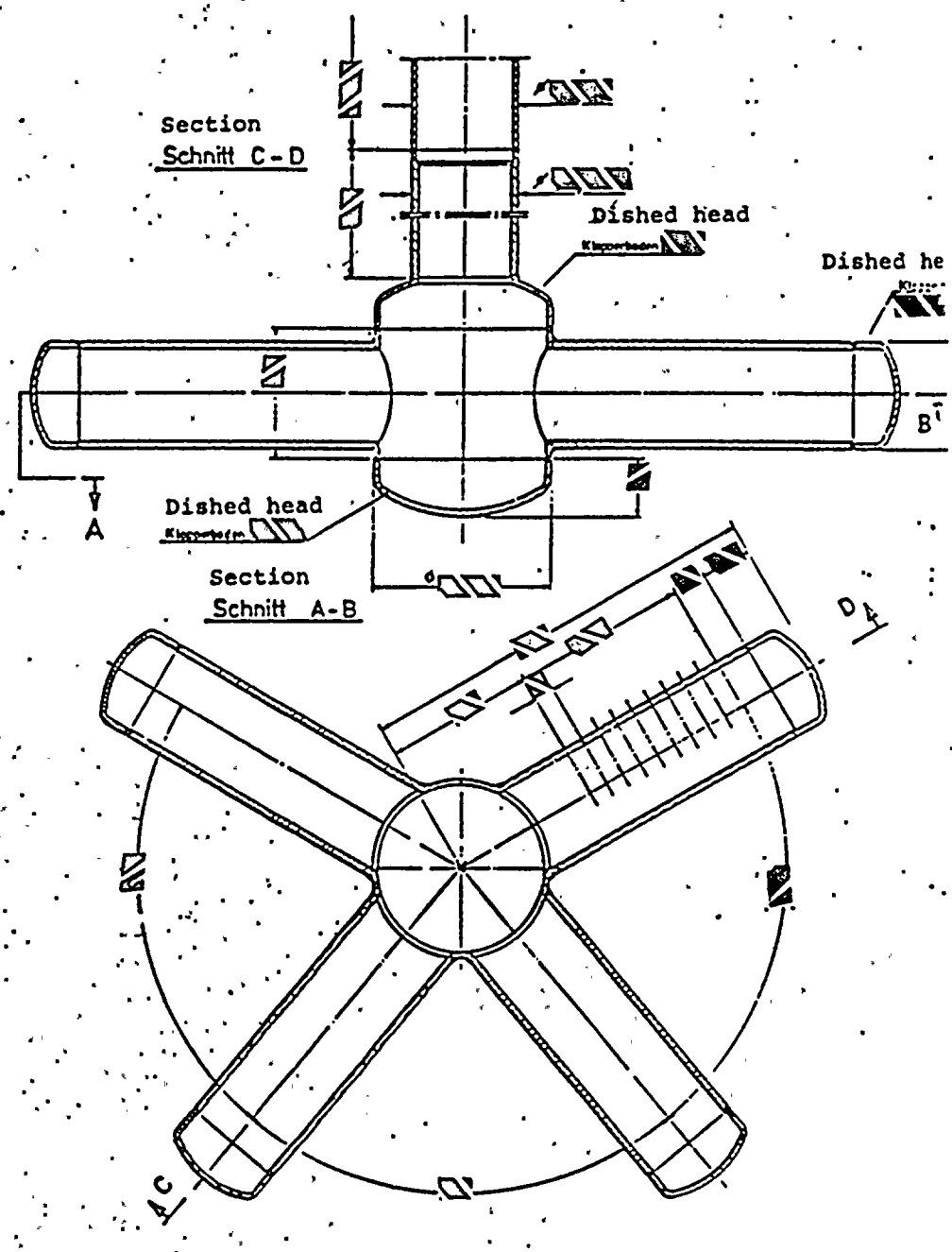

Bild 4.4 Figure 4.4

Lochrohrdüse HS 1 Perforated pipe quencher HS1

Modelldüse für GKM-Versuchsstand
Model quencher for GKM test stand

KRAFTWERK UNION AG PROPRIETARY INFORMATION

Figure..... 4.5 - 4.11

6-87 - 6-93

MODEL CONDENSATION TEST STAND

MODELL - KONDENSATIONS - VERSUCHSSTAND

High-pressure connection

Hochdruck-Anschluß

Arrangement and instrumentation

Anordnung und Instrumentierung

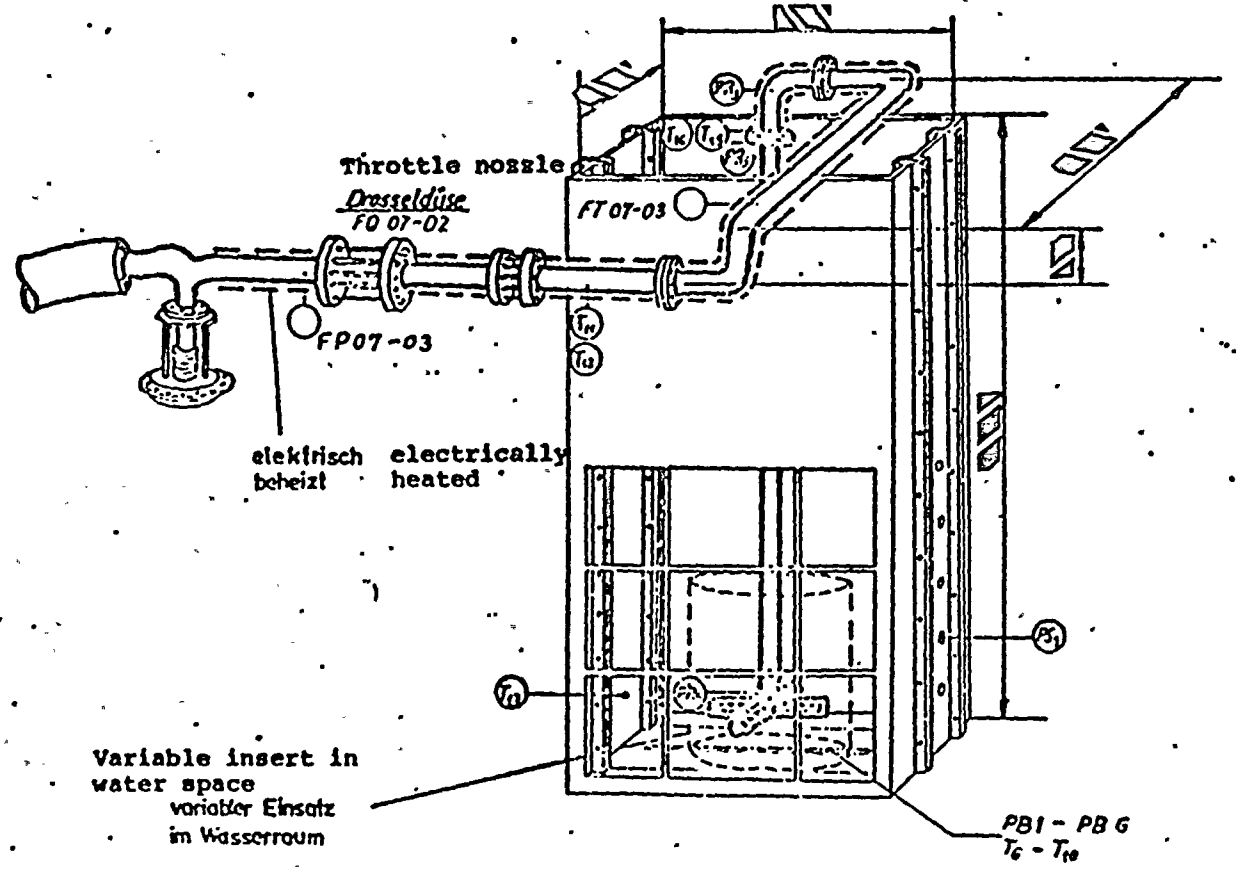

6-94

Bild 4.12

Figure 4.12

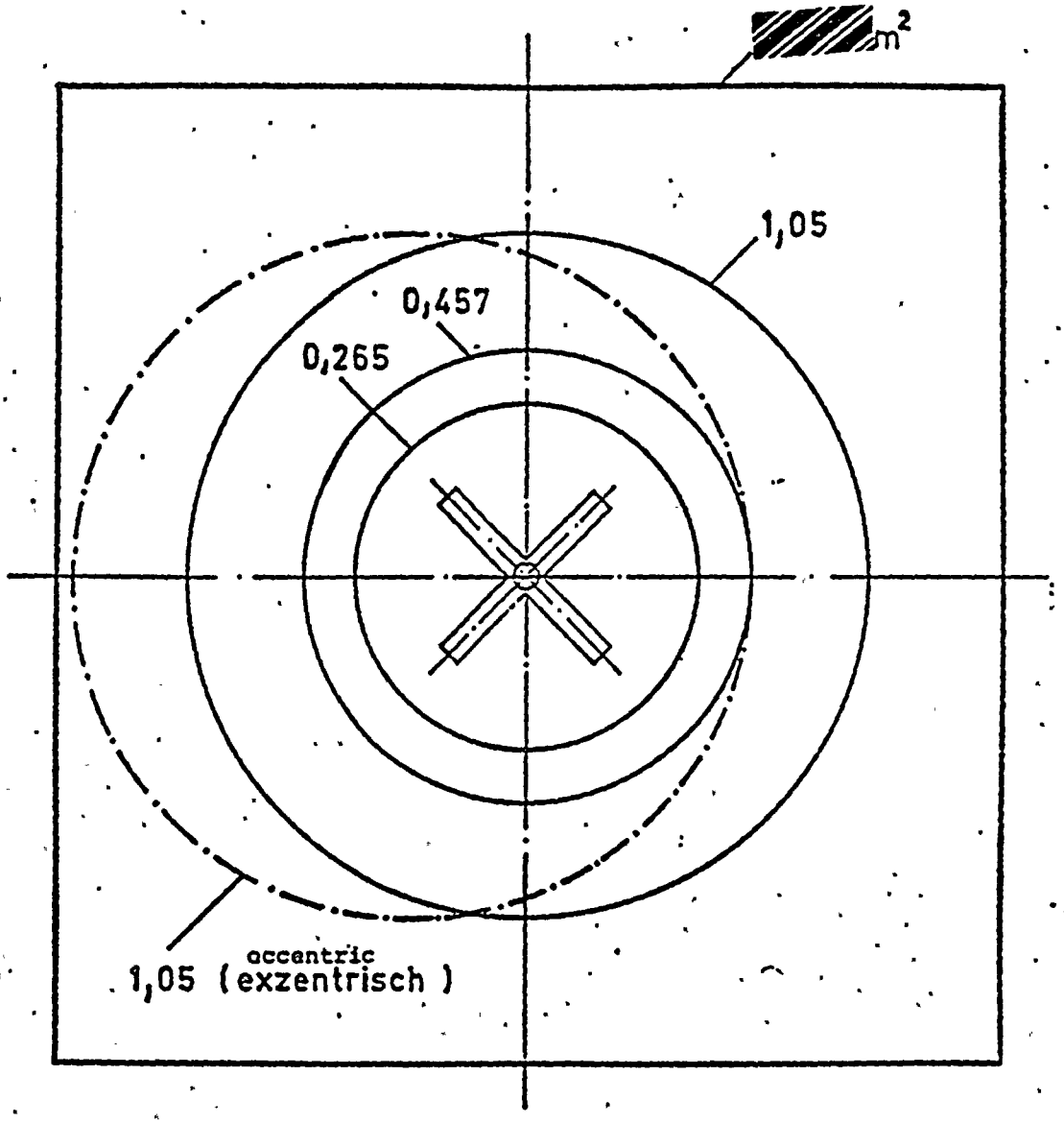

Bild 4.13 Figure 4.13

Einfluß der freien Wasserfläche
Versuchsaufbau im Modelltank in Gwh

Influence of free water-area
Set-up in the model tank in Gwh

KRAFTWERK UNION AG PROPRIETARY INFORMATION

Figure..... 4.14 - 4.26

6-96 - 6-108

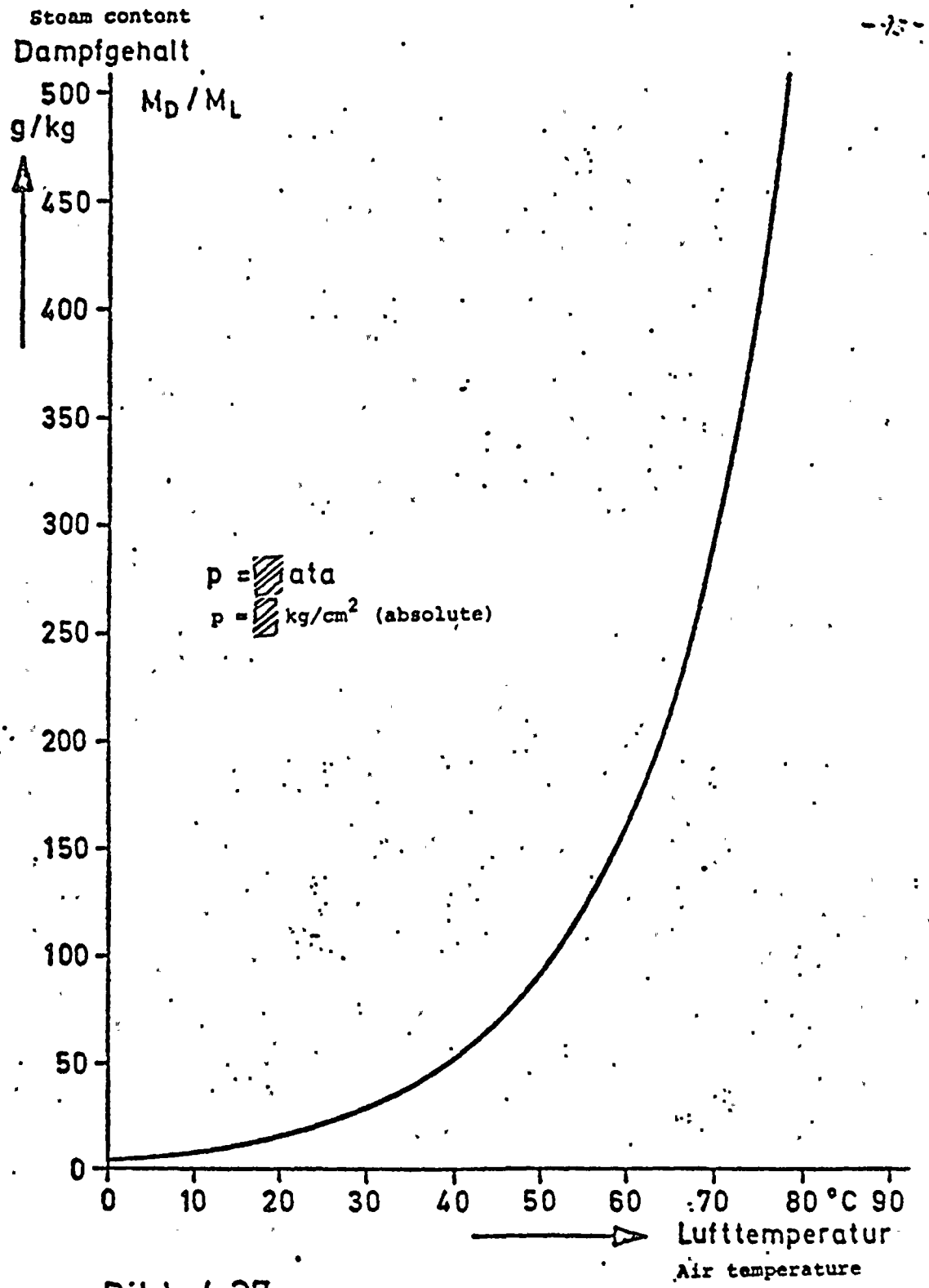

Bild 4.27 Figure 4.27

Dampfgehalt von gesättigter Luft

Steam content of saturated air

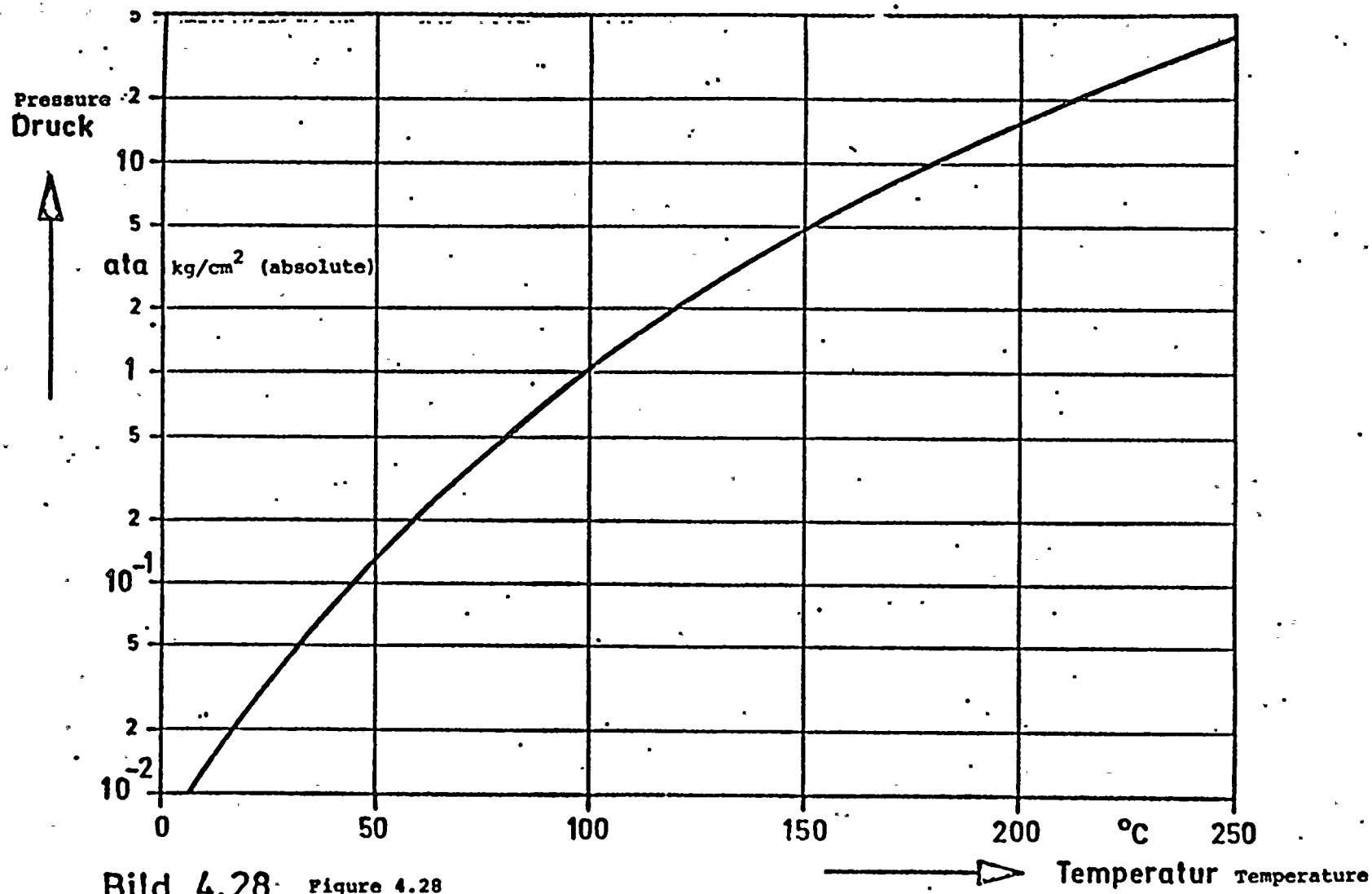

Bild 4.28 Figure 4.28

Dampfdruck in Abhängigkeit von der Temperatur für Sattdampf

Steam pressure versus temperature for saturated steam

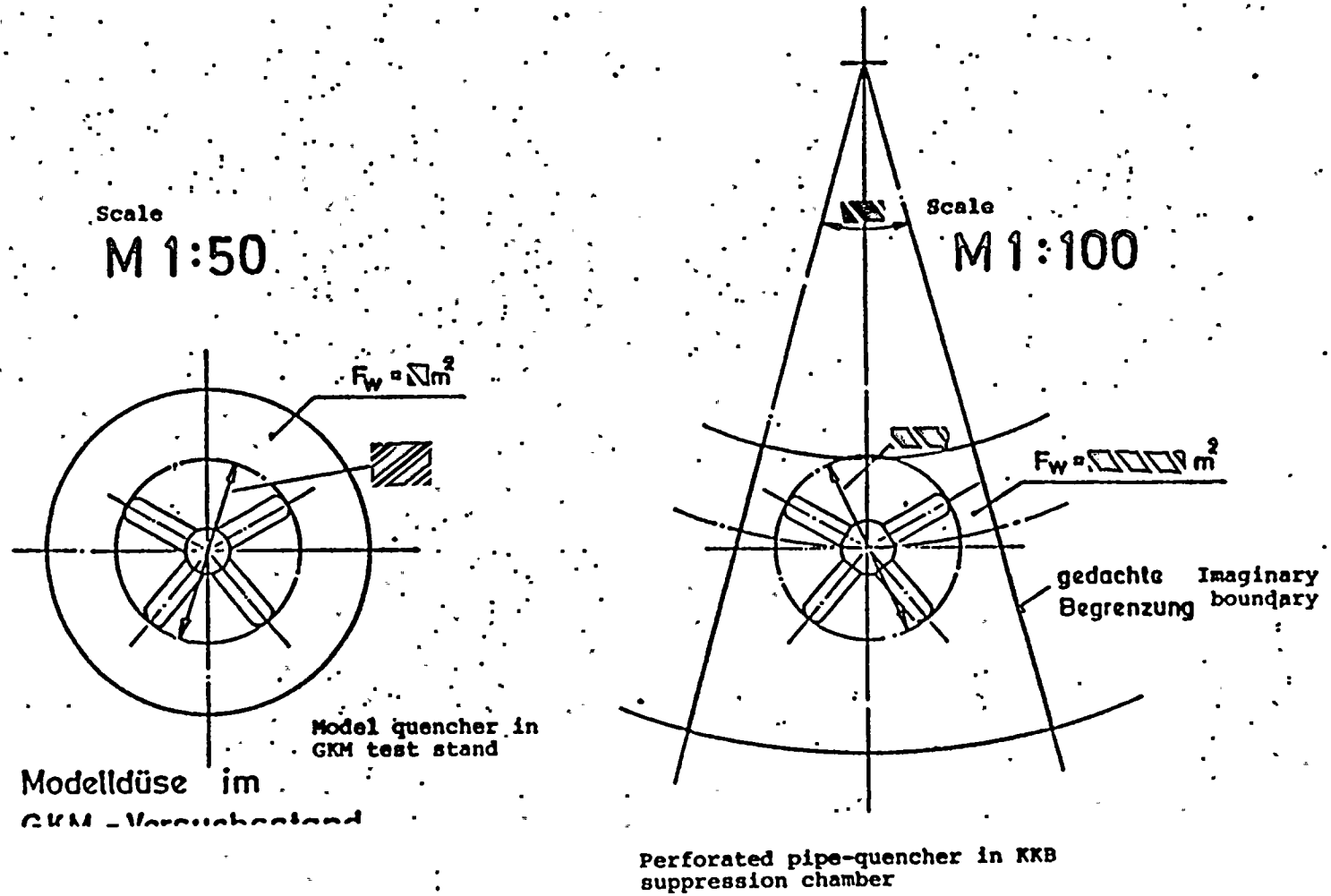

Figure 5.1

Comparison of perforated-pipe quencher in the test stand and in the KKB plant

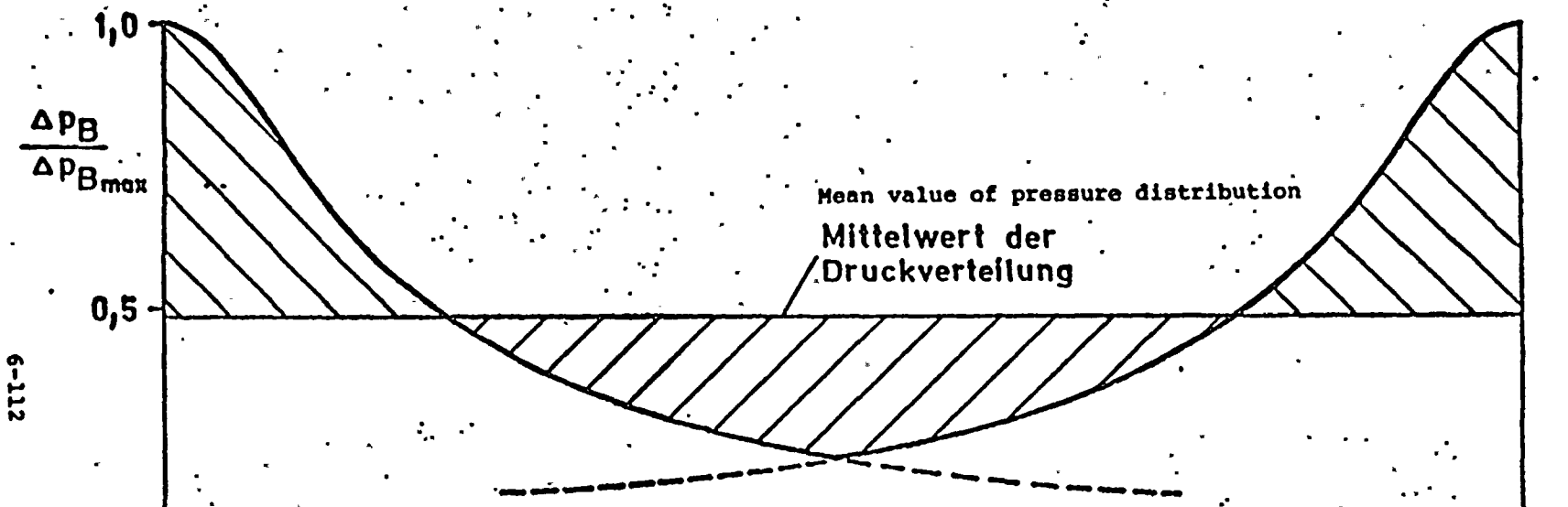

Bild 5.2 Figure 5.2

KKB-Umfangsverteilung der maximalen Bodenbelastung

KKB - Circumferential distribution of maximum bottom load

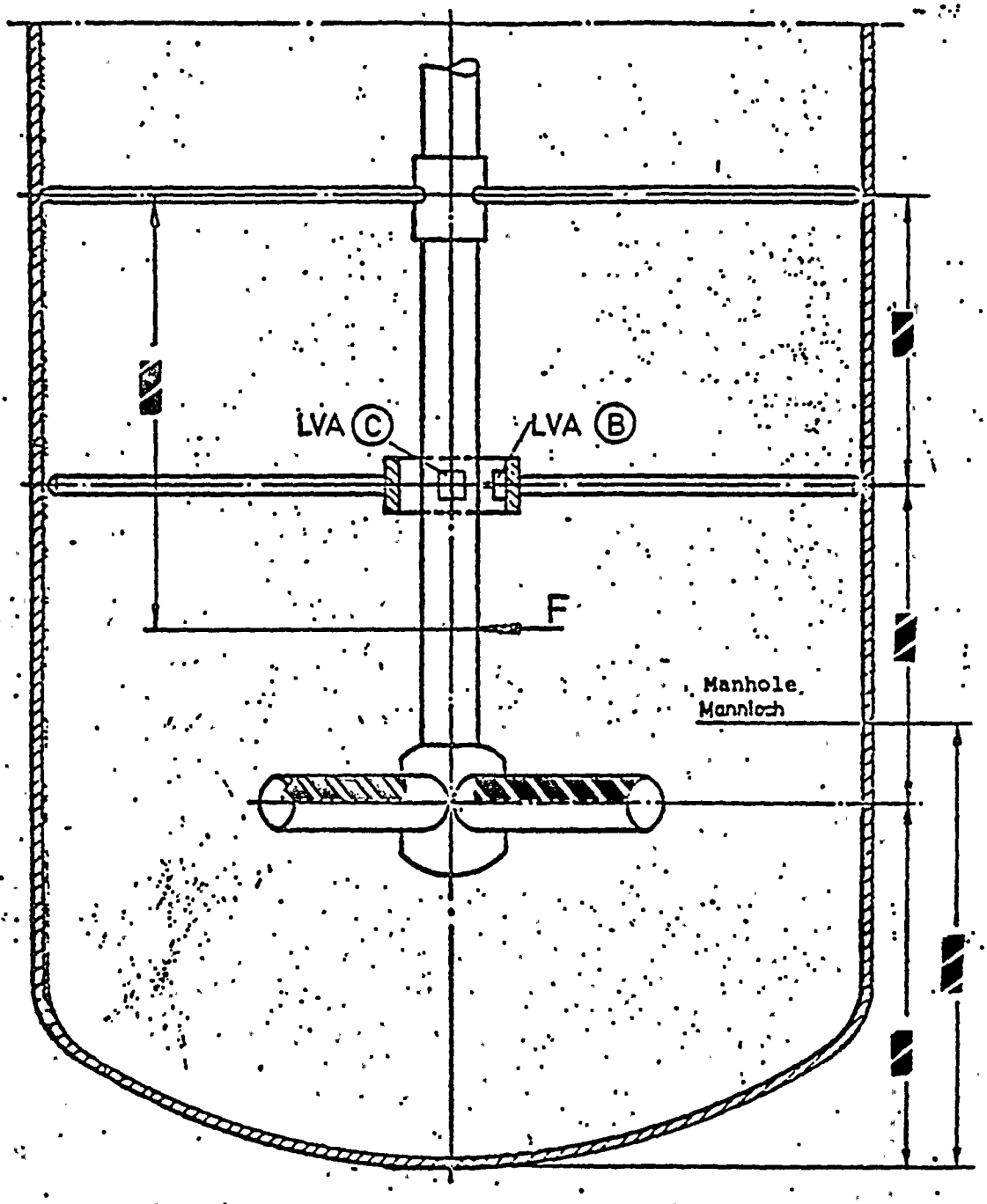

Bild 6.1 Figure 6.1

Arrangement and position of the linear displacement transducers

Anordnung und Lage der Längenverschiebungs-aufnehmer

(Meßebene I) (Measurement plane I)

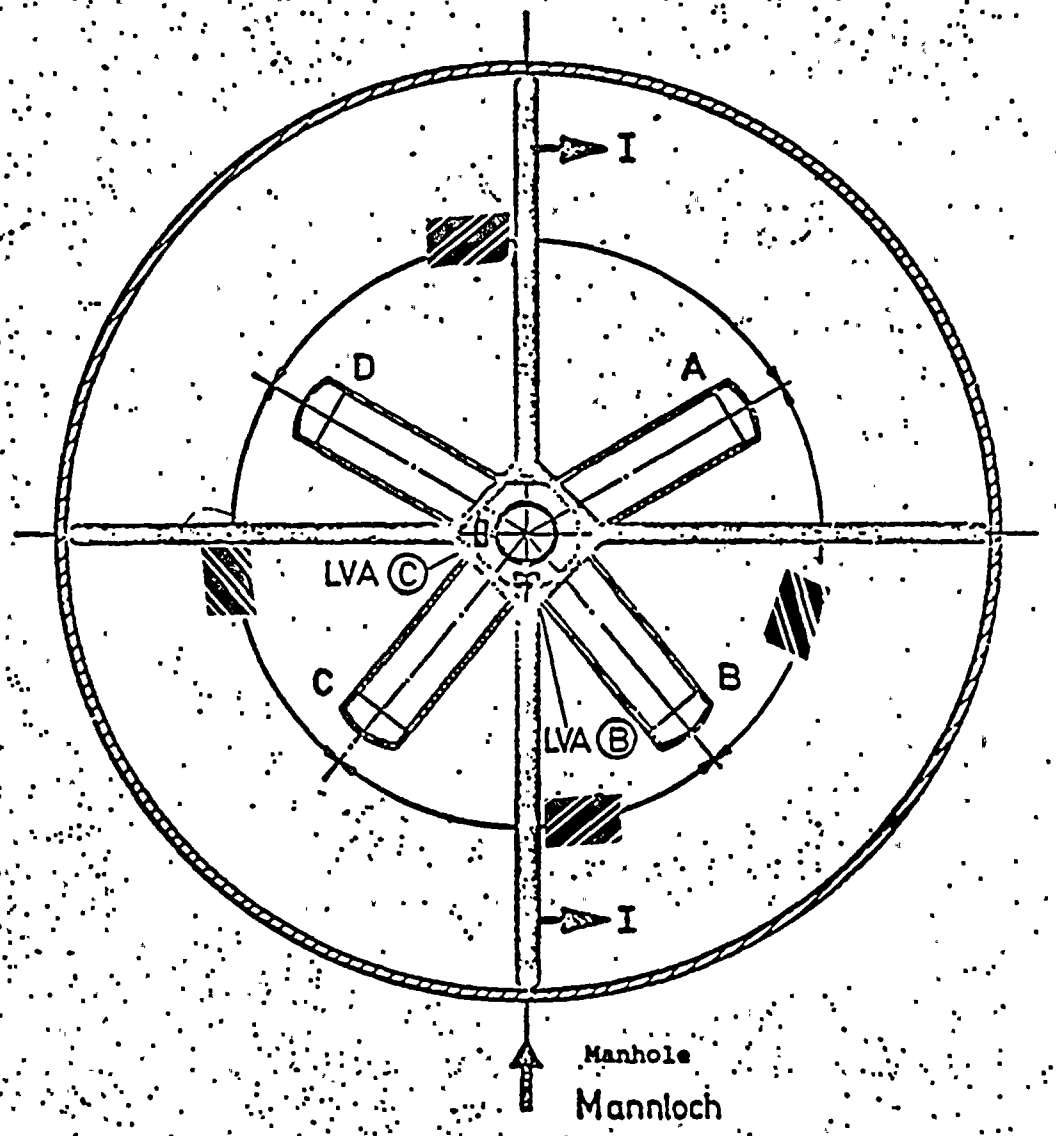

Bild 6.2 Figure 6.2

Anordnung der LVA's mit Einbaulage der Lochrohrdüse HS1 im GKM-Behälter

Arrangement of the linear displacement transducers with installation position of the perforated-pipe quencher HS1 in the GKM tank

KRAFTWERK UNION AG PROPRIETARY INFORMATION

Figure..... 6.3

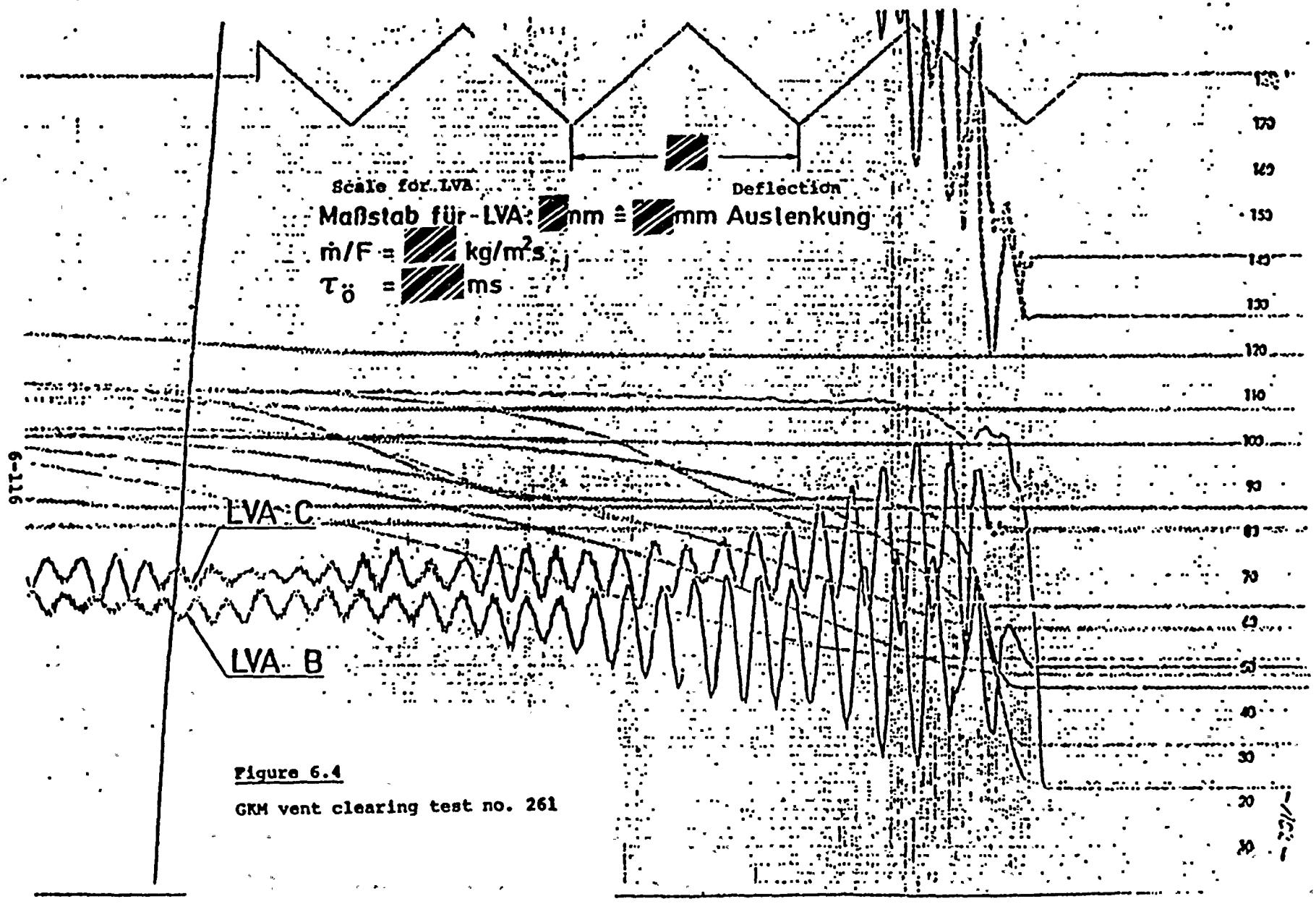

Figure 6.4

GKM vent clearing test no. 261

KRAFTWERK UNION AG PROPRIETARY INFORMATION

APPENDIX ..

6-117 through 6-136

REFERENCES

/1/ Weisshäupl, Slegers, Koch
KKB - Dynamic loading of the suppression chamber during relief processes
AEG-E3-2386 October 1972

/2/ Weisshäupl, Koch
Formation and oscillation of a spherical gas bubble under water
AEG-E3-2241 May 1972

/3/ Rumary, Smith, Smith
The Efficiency of a Water Pond for the Direct Condensation of Steam Air Mixtures, presented at the one-day discussion on direct contact heat transfer at the National Engineering Laboratory on 15th January, 1969

/4/ Becker, Frenkel, Melchior, Slegers
Construction and design of the relief system with perforated-pipe quencher
KWU-E3-2703 July 1973